Evaluation of Potential Post-Glacial Faults Using Bare-Earth LiDAR Topographic Data Near Ridley Island, British Columbia

Nicholas Novoa, L.G.

A report prepared in partial fulfillment of
the requirements for the degree of

Master of Science
Earth and Space Sciences: Applied Geosciences

University of Washington

December 2013

Project Mentor:
Mark Molinari, URS Corp.

Internship Coordinator:
Kathy Troost

Reading Committee:
Juliet Crider
Alison Duvall

MESSAGe Technical Report: 002

EXECUTIVE SUMMARY

I am presenting the results of my evaluation to identify topographic lineaments that are potentially related to post-glacial faulting using bare-earth LiDAR topographic data near Ridley Island, British Columbia. The purpose of this evaluation has been to review bare-earth LiDAR data for evidence of post-glacial faulting in the area surrounding Ridley Island and provide a map of the potential faults to review and possibly field check. My work consisted of an extensive literature review to understand the tectonic, geologic, glacial and sea level history of the area and analysis of bare-earth LiDAR data for Ridley Island and the surrounding region.

Ridley Island and the surrounding north coast of British Columbia have a long and complex tectonic and geologic history. The north coast of British Columbia consists of a series of accreted terranes and some post-accretionary deposits. The accreted terranes were attached to the North American continent during subduction of the Pacific Plate between approximately 200 Ma and 10 Ma. The terrane and post-accretionary deposits are metamorphosed sedimentary, volcanic and intrusive rocks. The rocks have experienced significant deformation and been intruded by plutonic bodies. Approximately 10 Ma subduction of the Pacific Plate beneath the North America Plate ceased along the central and north coast of British Columbia and the Queen Charlotte Fault Zone was formed. The Queen Charlotte Fault Zone is a transform-type fault that separates the Pacific Plate from the North America Plate. Within the past 1 million years, the area has experienced multiple glacial/interglacial cycles. The most recent glacial cycle occurred approximately 23,000 to 13,500 years ago. Few Quaternary deposits have been mapped in the area.

The vast majority of seismicity around the northwest coast of British Columbia occurs along the Queen Charlotte Fault Zone. Numerous faults have been mapped in the area, but there is currently no evidence to suggest these faults are active (i.e. have evidence for post-glacial surface displacement or deformation). No earthquakes have been recorded within 50 km of Ridley Island. Several small earthquakes (less than magnitude 6) have been recorded within 100 km of the island. These earthquakes have not been correlated to active faults. GPS data suggests there is ongoing strain in the vicinity of Ridley Island. The strain has the potential to be released along faults, but the calculated strain may be a result of erroneous data or accommodated aseismically. Currently, the greatest known seismic hazard to Ridley Island is the Queen Charlotte Fault Zone.

LiDAR data for Ridley Island, Digby Island, Lelu Island and portions of Kaien Island, Smith Island and the British Columbia mainland were reviewed and analyzed for evidence of post-glacial faulting. The data showed a strong fabric across the landscape with a northwest-southeast trend that appears to mirror the observed foliation in the area. A total of 80 potential post-glacial faults were identified. Three lineaments are categorized as high, forty-one lineaments are categorized as medium and thirty-six lineaments are categorized as low. The identified features should be examined in the field to further assess potential activity. My analysis did not include areas outside of the LiDAR coverage; however faulting may be present there. LiDAR data analysis is only useful for detecting faults with surficial expressions. Faulting without obvious surficial expressions may be present in the study area.

TABLE OF CONTENTS

LIST OF TABLES

LIST OF FIGURES

ACKNOWLEDGEMENTS

This report is one of the requirements for my capstone internship. The capstone internship is a graduation requirement for the Masters in Earth and Space Sciences, Applied Geoscience (MESSAGe) program at the University of Washington. The purpose of the capstone internship is to provide students with planning, data collection, analysis and writing experience working with a private or government employer. Each student finishes MESSAGe with a presentation of internship findings to a committee of faculty and professional mentors.

My internship project was performed in conjunction with work being performed by URS Corporation. My professional mentor is Mark Molinari, Senior Principal Engineering Geologist at URS. My faculty committee consists of the committee chair, Juliet Crider, Assistant Professor at the University of Washington, and the second reader, Alison Duvall, Assistant Professor at the University of Washington. Kathy Troost is the MESSAGe program coordinator with the University of Washington. Eric Stata, MESSAGe student, served as a peer reviewer for this report. I would like to thank all of them for guidance and feedback relating to the preparation of this report.

I appreciate the opportunity to be of service on this project.

1. INTRODUCTION

With this report, I present the results of my evaluation of potential post-glacial faulting using bare-earth light detection and ranging (LiDAR) topographic data near Ridley Island, British Columbia. The purpose of this evaluation was to review bare-earth LiDAR data for evidence of potential post-glacial faulting on Ridley Island and the surrounding area and provide a map of potential faults to review and field check in the future.

I obtained LiDAR data for Ridley Island as well as Digby Island, Lelu Island and portions of Kaien Island, Smith Island and the British Columbia mainland. The data was of sufficient density and vertical accuracy to generate 1m topographic contour maps of the study area. Ridley Island is located along the western coast of Canada, near Prince Rupert, British Columbia (Fig. 1). The Hecate Strait is located adjacent to the west coast of Ridley Island. Haida Gwaii, also known as the Queen Charlotte Islands, is located approximately 90 km west of Ridley Island. The state border of Alaska is located approximately 55 km north of Ridley Island. The area where LiDAR data is available is herein referred to as the study area (Fig. 2). Ridley Island is located south of Kaien Island and southwest of Digby Island. Lelu Island and Smith Island are located southwest of Ridley Island. The study area includes two small portions of the British Columbia mainland, one located northeast of Digby Island and the other located northeast of the Lelu and Smith Islands. The mainland area located northeast Digby Island is herein referred to as the northern B.C. mainland. The mainland area located northeast of Lelu and Smith Islands is herein referred to as the southern B.C. mainland.

Ridley Island is owned by the government of Canada and operated by the Prince Rupert Port Authority. Ridley Island is located south of Kaien Island, where the city of Prince Rupert is located, and can be accessed by existing roads and rail lines from Kaien Island or by boat. Ridley Island is approximately 4.1 km long by 2.0 km wide. Elevations on Ridley Island vary from sea level to approximately 45 meters above mean sea level. The northwest portion of the island is currently occupied by Prince Rupert Grain Limited and Ridley Terminals, Inc. The rest of the island is unoccupied.

Port Edward is located on the British Columbia mainland east of Ridley Island, partially in the study area. There is also a small airport located on Digby Island. There is a small community, known as Osland, along the southeast coast of Smith Island, outside of the study area. Lelu Island and the northern B.C. mainland appear to be undeveloped.

2. SCOPE OF WORK

My scope of services for this evaluation consisted of the following tasks:

- Review of readily available background data, including geologic data, geologic literature, geologic maps, topographic maps, GIS data, seismic hazard maps and literature relevant to the subject site.
- Evaluation of the glacial and sea level history of Ridley Island and the surrounding area.
- Review and analysis of LiDAR data made available to me by Mr. Mark Molinari.

- Preparation of several GIS map products including a topographic contour map, slope map, aspect map, and hillshade map to aid in identifying potential post-glacial faults in the study area.
- Preparation of a potential post-glacial fault map identifying potential post-glacial faults in the study area and ranking the potential faults from low to high regarding the likelihood that they are related to post-glacial faulting.
- Provide recommendations for field verification of the identified potential post-glacial faults.
- Preparation of this report summarizing the information obtained, analyses performed, and recommendations regarding potential post-glacial fault hazards in the study area.

3. GEOLOGIC SETTING

The central and northern portions of western British Columbia consist of a series of accreted terranes. Approximately 200 million years ago (Ma), the Pacific Plate began subducting under the North America Plate along northern and central British Columbia (Gottesfeld, 1985). Subduction continued along the north coast of British Columbia until about 10 Ma (Gottesfeld, 1985). During the subduction process, additional material nearly 300 km wide was accreted onto the North America Plate (Gottesfeld, 1985). Subduction of the Pacific Plate ceased along the central and north coast of British Columbia approximately 10 Ma and the Queen Charlotte Fault Zone (QCFZ) was formed (Gottesfeld, 1985). The QCFZ is a transform fault that separates the Pacific Plate from the North America Plate. The QCFZ consists of right-lateral, high angle northwest-southeast trending faults. Today, seismic activity along the north coast of British Columbia is dominated by movement along the QCFZ. Few earthquakes have occurred within the mainland of British Columbia near the north coast (Clague, 1984; Advanced National Seismic System, 2013).

The study area is located along the coast of west-central British Columbia. The study area is part of the coastal trough and Coast Mountain area of the Western System physiographic area (Clague, 1984). In the vicinity of the study area, the coastal trough is known as the Hecate Lowland (Clague, 1984). The majority of the study area is located within the Hecate Lowland, near the eastern edge (Clague, 1984). The Hecate Lowland is a 15-40 km wide, low-lying strip of the coast that extends for approximately 600 km along the Coastal Trough (Clague, 1984). The Hecate Lowland is bordered by the sea and elevations in the lowland do not exceed a few hundred meters (Clague, 1984). A portion of the southern B.C. mainland and Kaien Island are considered part of the Coast Mountain area (Clague, 1984).

According to geologic mapping conducted by the British Columbia Geological Survey (Cui et al., 2013), Ridley Island, Kaien Island, Lelu Island, and portions of the British Columbia mainland, Digby Island and Gravina Island are underlain by the Gravina assemblage (Geologic map symbol: JKGms). The Gravina assemblage consists of post-accretionary, Jurassic to Cretaceous lower amphibolite/kyanite grade, metamorphosed volcanic-rich turbidites. A portion of Digby Island and a portion of the British Columbia mainland located in the northern study area are underlain by the Moffatt Volcanics (Geologic map symbol: lmJMv). The Moffat Volcanics consist of Lower Jurassic to Middle Jurassic basalt and rhyolite. The Descon

Formation (Geologic map symbol: ODmv) and the Mathieson Channel Formation (Geologic map symbol: DMCcg1) also underlie a portion of Digby Island. The Descon Formation consists of Early Ordovician greenschist to amphibolite grade volcanic and volcaniclastic rocks from the Alexander Terrane. The Mathieson Channel Formation consists of Lower Devonian conglomerates and sandstones from the Alexander Terrane. Smith Island is underlain by the Captain Cove Plutonic Suite (Geologic map symbol: EKCqd) and the Kumealon unit (Geologic map symbol: lPms). The Captain Cove Plutonic Suite consists of Mid-Cretaceous quartz diorite and granodiorite. The Kumealon unit consists of Lower Devonian metaclastics from the Alexander Terrane. A portion of the geologic map shapefile released by the British Columbia Geological Survey showing these rock units is reproduced in Figure 3.

As noted above, much of the study area is underline by rocks of the Gravina assemblage. The Prince Rupert Shear Zone separates the Gravina assemblage from older geologic units located to the west (Fig. 4). To the northeast, the Gravina assemblage is separated from rocks of the Endicott Arm assemblage by the Coast Shear Zone (Fig. 4). A structural map of the Prince Rupert area prepared by Chardon (2003) show foliations in the study area trending northeast-southwest dipping to the northeast at angles of 0 to 60 degrees (Fig. 5). The dips of the foliations appear to increase from west to east (Fig. 5). Around the northern B.C. mainland and the northern end of Kaien Island the foliations curve and become oriented north-south (Fig. 5).

North America has seen repeated glacial and interglacial cycles over the last 2 to 3 million years (Gottesfeld, 1985). These glaciations have altered the topographic landscape of the continent. There have been at least a half dozen recorded glacial advances that have extended across western and southern British Columbia and extended into the Puget lowland in the State of Washington (Booth et al., 2003). The most recent glacial cycle was known as the Frasier Glaciation. The Frasier Glaciation began around 25,000 to 30,000 years before present (BP) and ice reached its maximum extent in the study area 17,000 to 16,000 years BP (Clague, 1984; Warner et al. 1982). Glaciers advanced from the mountains and spread westward down the valleys toward the coast. Figure 6 is a reproduction of the pattern of glacial flow during the Frasier Glaciation from the Geological Survey of Canada (Clague, 1984). The major ice sheets came out of the Skeena River valley to the south and the Nass River valley to the north in the study area region (Clague, 1984). Recognition of the direction of flow across the study area is important because glaciers can leave topographic lineaments and fabrics that are visible in bare-earth LiDAR data. According to information published by the Geological Survey of Canada, there are few recessional deposits and landforms in the study area and only a thin cover of late Pleistocene deposits present (Clague, 1984).

4. BACKGROUND

Isostatic depression and rebound coupled with changing eustatic sea levels have created spatially variable changes in relative sea level along the British Columbia coastline (Barrie and Conway, 2002; Barrie and Conway, 1999; Hetherington et al., 2003). A study by Archer (1998) shows that the relative sea level at Port Simpson, located approximately 27 km north of Prince Rupert, was approximately 50 +/- 2 meters above present levels about 12,500 years BP and returned to near present-day sea levels about 7,500 years BP.

Paleoshorelines can be recorded along coastlines in the form of marine terraces. A marine terrace is a relatively flat surface created by wave activity. Marine terraces may be visible in the study area as planar features along the coast and deformed terraces can be indicators of fault-related movement. The study by Archer (1998) suggests marine terraces formed after the most recent glaciation in the vicinity of the study area should not be present at an elevation above approximately 50 meters. Additional post-glacial marine terraces may be present below 50 meters. Displacement or deformation of the post-glacial marine terraces, if present, may be indicative of post-glacial faulting. Additional planar features or terraces may be present above 50 meters. These terraces may be related to older paleoshorelines, tectonic uplift, or glacial processes. The post-glacial and older terracing can provide a useful way to constrain timing of faulting or deformation if the terraces can be associated with known events.

Numerous faults have been mapped around the study area. Figure 4 shows faults identified by the B.C. Ministry of Energy and Mines (Massey et al., 2005). The main faults identified in the vicinity of the project are the Prince Rupert Shear Zone, Coast Shear Zone and Lampost Fault. Unfortunately, the data from Massey et al. (2005) does not include any data regarding the last time of displacement or activity along the faults. The Coast Shear Zone is located approximately 12.8 km northwest of the study area. The Coast Shear Zone is up to 10 km wide and experienced reverse motion between 65 Ma and 57 Ma and normal motion between 57 Ma and 50 Ma (Gehrels et al., 2009). According to research published by Davidson et al. (2003), the most recent movement along the Coast Shear Zone occurred as dextral strike-slip displacement approximately 29.8 Ma based on Ar-dating of pseudotachylyte. The Coast Shear Zone may have formed as part of the southern continuation the Denali Fault approximately 67 Ma (Gehrels et al., 2009). The Denali Fault is a historically active fault and the Coast Shear Zone merges with the Denali Fault in southeast Alaska (Gehrels et al., 2009). There is no significant historical seismicity recorded or published data indicating post-glacial activity on the Coast Shear Zone. Studies suggest the Prince Rupert Shear Zone was active prior to approximately 90 Ma based on structural relationships and timing of metamorphic events (Crawford et al., 1999; Granger, 2001). Mineral lineations and shapes of boudinage zones suggest the shear zone experienced primarily strike-slip movement although mapping by the British Columbia Geological Survey classify portions of the shear zone as a thrust fault around the study area (Crawford et al., 1999; Granger, 2001; Cui et al., 2013). Research by Angen (2013) indicates the Lampost Fault was active during the mid-Cretaceous. The Lampost shear zone is 50 to 100 meters wide and experienced sinistral-normal shear based on shear sense indicators (Angen et al., 2012). Published data does not indicate the presence of any significant active faults within 50 km of the project site (Crawford et al. 1999, Granger, 2001; Angen, 2013; Nelson et al. 2012; Massey et al., 2005).

Figure 7 shows the seismicity that has been recorded in the region since 1898 (Advanced National Seismic System, 2013). The majority of seismicity around the north coast of British Columbia occurs along the QCFZ. The Queen Charlotte Fault Zone is capable of producing earthquakes > Mw 8 (Wesson et al., 1999). The largest historical earthquake generated by the QCFZ was a magnitude 8.1 quake in 1949 (Wesson et al., 1999). Most recently, magnitude 7.8 and 8.5 earthquakes occurred along the QCFZ on October 28, 2012 and January 5, 2013, respectively (Advanced National Seismic System, 2013). The mainland area near Prince Rupert was considered aseismic until 1973, when a magnitude 4.7 earthquake occurred 20 km southwest

of Terrace (Clague, 1984). Several earthquakes with magnitudes of less than 4.0 have been recorded in the vicinity of the study area (Fig. 7). The closest recorded earthquake to the study area is located approximately 50 km to the north in southeast Alaska. The earthquake had a magnitude of 4.5 (Advanced National Seismic System, 2013). The closest recorded earthquake greater than a magnitude 5.0 is located approximately 88 km southwest of the study area in the Hecate Strait (Fig. 7). The earthquake catalogue does not include information about the association of a specific earthquake with a specific fault.

The lack of seismicity and known active faults does not eliminate the possibility for significant earthquakes to occur in or around the study area. Known faults currently thought to be inactive may have long-recurrence intervals and not experienced movement in recorded history. Additionally, there is a possibility that unknown faults exist in or near the study area that may represent a hazard to the area. New faults are continually being discovered around the U.S. and Canada (Conway et al., 2012; Haugerud et al., 2003; Howle et al., 2012; Thackray et al., 2013). Two increasingly popular tools used to help discover new or newly active faults are LiDAR and Global Positioning System (GPS) data. GPS and LiDAR are discussed in more detail below.

With GPS, scientists have been able to perform detailed measurements of plate motions at fixed location stations. The strain rate can be calculated by comparing the relative movement of adjacent stations with respect to time. Strain is a dimensionless measure of the deformation. Several studies have been conducted examining strain rates along the western coast of Canada (Mazzotti et al., 2003a, 2003b, 2008, 2011; Leonard et al., 2007). These studies compare the relative motions recorded by GPS stations and calculated strain rates to the known tectonics, seismicity and seismic hazards in the region. Mazzotti et al. (2008, 2011) and Leonard et al. (2007) used the measured the amount of deformation in the crust of the earth using GPS stations to calculate regional strain rates. Studies by Mazzotti et al. (2008, 2011) and Leonard et al. (2007) show an accumulation of strain in the area between the north coast of British Columbia and the QCFZ. In general, the area west of the Hecate Strait is moving faster to the north than the area east of the Hecate Strait (Mazzotti et al., 2008). This is creating right-lateral shear in the area of the Hecate Strait. Based on the GPS measurements, the shear is accumulating at a rate of approximately 5 mm/yr over a 300 to 400 km wide area from the Queen Charlotte Islands to the Coast Mountains (Mazzotti et al., 2008). There is also a small component of margin-normal shortening occurring in the region (Mazzotti et al., 2008). The accumulation of strain must be accommodated in the crust. This may occur through aseismic deformation, seismic faulting, or some combination of the two. In the case of faulting, the most obvious way to accommodate the right-lateral shear in the study area region would be right-lateral strike slip displacement along northeast-southwest trending faults. The northeast-southwest directed shortening could be accommodated by reverse slip along northwest-southeast trending faults located along the eastern portion of the Hecate Strait and in the western Coast Mountains. The exact nature of faulting, if present, will be controlled by the geology, lithology and crustal conditions in the area.

The studies by Mazzotti et al. (2008, 2011) and Leonard et al. (2007) have shown that current probabilistic seismic hazard assessments based solely on historical seismicity rates may underestimate the seismic hazard along the north coast of British Columbia by a factor of 1.5 to 3 compared to rates implied by GPS velocities. However, Mazzotti et al. (2008) warns that similar GPS studies have typically seen a systematic overestimation of strain rates. Two possible

explanations for the systematic overestimation are 1) that some of the strain may be accommodated aseismically and 2) that current seismic catalogues are incomplete or inaccurate due to unknown sources and inaccurate source parameters (Mazzotti et al, 2008). Nevertheless, the high strain rates in the vicinity of the study area calculated by Mazzotti et al. (2003a, 2003b, 2008, 2011) and Leonard et al. (2007) raise additional concerns about unknown seismic sources in western British Columbia that could increase the seismic ground motion hazard in the vicinity of the study area.

5. METHODS

One of the most common approaches today to identify active faults in an area is topographic analysis of bare-earth LiDAR data (Haugerud et al., 2003; Howle et al. 2012; Thackray et al, 2013). Analysis of topographic images created by bare-earth LiDAR data, known as digital elevation models (DEMs), has become an increasingly common tool to locate previously unknown faults.

LiDAR has many advantages over previous measurement techniques. LiDAR is a remote sensing technology and can cover large areas in a short period of time. LiDAR also has the unique ability to "remove" the vegetation cover from the terrain. LiDAR data is collected by transmitting light pulses and recording return times. The transmitted light pulse diffuses and reflects off of multiple surfaces. The return times from each different surface is recorded. Unless very dense vegetation is present, we can assume that the last return is reflecting off the ground and not the vegetation above. By using only the last returns and some interpolation, it is possible to calculate the approximate elevation of the ground surface. The resulting data with the vegetation removed is known as a bare-earth image. The x and y coordinates are determined from the known azimuth and angle of the laser pulse. By tying the measurements into a known coordinate system using GPS measurements made during LiDAR data acquisition, the latitude, longitude and elevation of each measurement are determined. The resulting data can be viewed as raster images in GIS programs. By removing vegetation, it is possible to see geologic features (e.g. faults and landslides) and anthropogenic features (e.g. ruins and roads) in areas where vegetation would normally prevent us from doing so.

LiDAR data was acquired from a private company as part of an ongoing study by URS. Data coverage includes Ridley Island, Digby Island, Lelu Island and portions of Kaien Island, Smith Island and the British Columbia mainland. The original LiDAR data sets were collected for other projects not related to this study. For my study, I was provided with bare-earth LiDAR data in the form of seven 1-meter gridded DEM files (Mark Molinari, URS, digital files, 2013). The original LiDAR data was collected using a first-return density of approximately 3-4 points per square meter. The LiDAR data was collected from May 24-25, 2012.

As part of my scope of work, I reviewed and analyzed the available LiDAR data for evidence of post-glacial faulting in the study area. As part of my analysis, I combined the LiDAR data sets into one master DEM raster file (Fig. 8). I used the master DEM file to create four shaded relief raster files, known as hillshades. Each hillshade file was generated using a different solar illumination angle: 45, 135, 225, and 315 degrees. Four hillshades were created because the azimuth of the solar illumination angle creates biased shading based on the azimuth angle. By

utilizing the four different hillshades, features became more or less pronounced. The four hillshade files were made partially transparent and overlayed on top of each layer to eliminate preferential shading from one solar orientation in order to do a first-pass assessment (Fig. 9). The master DEM file was also used to generate slope, aspect and topographic contour maps (Figures 10 – 12).

LiDAR data analysis was conducted to identify linear topographic anomalies within the study area. Linear topographic anomalies are linear features visually identified as distinct or anomalous changes in topography. The DEM, hillshade, slope, topographic contour and aspect maps were each visually reviewed for signs of linear features. In the hillshade image, linear features appear as shaded lineations. These features were identified using the four separate hillshade images as well as the composite image. Linear features were identified in the slope map by sharp changes in slope angle. Linear features can be identified in the contour map using changes in the spacing between contours or sharp changes in the direction of contours. 1-, 5- and 10-meter contour intervals were used while trying to evaluate potential scarps, lateral offsets and other subtle geomorphic features such as small terraces and shorelines. A 50-meter contour interval is shown in Figure 9 for display purposes only. Linear features were identified in the aspect map by changes in aspect. Each of the images and maps were continuously displayed, reclassified and rotated through while identifying the lineaments.

Not all linear features are potential faults. A variety of geologic processes can create topographic linear features including, but not limited to, glacial flow, relict shorelines, fractures, geologic contacts, preferential weathering or erosion along geologic beds, glacial landforms and deposits, fluvial landforms and deposits, and hillslope processes. Glacial landforms and deposits, such as lateral moraines, medial moraines, eskers, striations and drumlins, would most likely be parallel to sub-parallel to the direction of glacial flow. Other glacial landforms and deposits, such as terminal moraines, kames, kettles, glacial erratics and outwash deposits, may be irregularly shaped or not be dependent on the direction of glacial flow. Relict shorelines would most likely be manifested as relatively flat platforms parallel to the coastline, unless they have been deformed after deposition. Based on analysis of recent sea level change in the area, post-glacial marine terraces are not expected above an elevation of about 50 meters. Given the age and complex history of rocks in the study area, fractures may present in the study area and appear as linear features without a preferential orientation. Geologic contacts and preferential weathering and erosion along geologic beds would manifest itself as linear features parallel to bedding and contacts. Fluvial landforms and deposits would most likely be parallel to sub-parallel to the direction of stream flow. Hillslope processes, such as slope failures, can manifest themselves as linear features oriented downslope or sub-parallel to the slope face. One other factor of note that can shape the topographic landscape is anthropogenic processes and features. These processes and features, such as grading, structures and roads, do not have preferential orientation directions, but may be linear and are identifiable in hillshade images.

Using the DEM, hillshade, slope, topographic contour and aspect maps, linear topographic anomalies were visually identified and traced in ArcGIS. Given the extensive visual fabric seen across the study area, not all linear topographic anomalies were identified and traced in ArcGIS. Only those features that may be related to faulting are marked as potential post-glacial faults. In general, obvious drainage channels and anthropogenic features were not included in the

identified lineaments, as well as any feature that was less than 1 km long or displayed sharp orientation changes of approximately 30 degrees or more. Lineaments less than 1 km long if the lineament appear to be a splay of a longer lineament or if the lineament was cut-off due to the extents of the LiDAR data or the presence of water. Each of the identified lineaments was categorized into one of three categories: Low, Medium or High. These categories represent the relative likelihood of the lineaments being a potential post-glacial fault based on the visual analysis. Known or possible faults should be considered active if they have experienced post-glacial displacement or may experience displacement in the future. In general, features classified as "high" displayed signs of lateral offset across the potential fault. Features that are classified as "low" displayed characteristics that could be related to faulting or explained by the geologic processes described above. Features classified as "medium" are generally the same as low features, but are more visually pronounced in the DEM, hillshade, slope, contour and/or aspect maps or exceed 4.0 km in length. The resulting map is presented in Figure 13 with regional blow-up maps shown in Figures 14, 15, and 16.

6. RESULTS

Analysis of the bare-earth LiDAR data resulted in the location of eighty (80) potential post-glacial faults in the study area (Fig. 13). The total length of all potential post-glacial faults identified is 138.6 km. The minimum potential fault length is 0.25 km and the maximum potential fault length is 10.2 km. The mean potential fault length is 1.7 km. Three of the potential faults are categorized as high, forty-one of the potential faults are categorized as medium, and thirty-six of the potential faults are categorized as low. The statistics for each potential post-glacial fault category are summarized in Table 1 below. A breakdown of the potential post-glacial fault locations by category is presented in Table 2 below.

Table 1 – Summary of Statistics for Each Category of Potential Post-glacial Faults

Category	No. of Potential Faults	Minimum Length (km)	Maximum Length (km)	Average Length (km)	Total Length of All Potential Faults (km)
High	3	1.2	2.4	1.7	5.1
Medium	41	0.4	10.2	2.0	83.9
Low	36	0.25	3.8	1.4	49.6

A total of three high category potential post-glacial faults were identified (Fig. 13). One of the high category potential faults is located at the southwest corner of Ridley Island (Fig. 15). The potential fault is oriented northwest-southeast and shows signs of right-lateral offset. The second of the high category potential faults is located on the southern portion of Kaien Island (Fig. 15). The potential fault is oriented approximately east-west and appears to offset streambeds with a left-lateral sense of slip. The third high category potential fault is located on the north-central portion of Smith Island (Fig. 16). The potential fault is oriented northeast-southwest and displays signs of right-lateral offset.

Table 2 – Breakdown of Potential Post-Glacial Fault Locations by Category

Location	No. of Low Category Potential Faults	No. of Medium Category Potential Faults	No. of High Category Potential Faults
Ridley Island	4	4	1
Kaien Island	1	15	1
Lelu Island	--	3	--
Smith Island	4	7	1
Digby Island	1	6	--
Northern B.C. Mainland	13	--	--
Southern B.C. Mainland	13	6	--

A total of forty-one medium category potential post-glacial faults were identified (Fig. 13). Five of the medium category potential faults exceed 4.0 km in length. The medium category potential faults are primarily oriented northwest-southeast to north-south. Approximately eleven of the medium category potential faults are oriented northeast-southwest to east-west.

A total of thirty-six low category potential post-glacial faults were identified (Fig. 13). The low category potential faults are primarily oriented northwest-southeast to north-south. Approximately ten of the low category potential faults are oriented northeast-southwest to east-west.

7. DISCUSSION

Figure 9 reveals a perceptible northwest-southeast trending fabric across much of the study area. The fabric appears to mirror the foliations shown on the structural map of the Prince Rupert area (Fig. 5). The fabric shown in figure 9 is not consistent with the glacial flow direction from the most recent glaciation (Fig. 6). This suggests the most recent glaciation may not have played a major role in the shaping of the study area. Anthropogenic structures and influences on the topography can clearly be identified around the north end of Ridley Island (Fig. 15). Additional anthropogenic features can also be identified on Kaien Island, Digby Island and around the northern portion of the southern B.C. mainland area. There are no major fluvial landforms observed in the study area, but numerous small drainage channels can be observed along the slopes of the study area.

As stated above, a total of 80 potential post-glacial faults were identified using the LiDAR data. The majority of potential faults identified are parallel to sub-parallel the foliation orientation mapped in the area. These potential faults may be related to the processes that created the foliations. The high and medium category potential faults identified at the southwest corner of Ridley Island may be part of the Prince Rupert Shear Zone. The fault locations shown on Figure 4 are not considered accurate at a scale of less than 1:250,000 and, therefore, should be not used for precise locating of the faults.

A number of the potential faults identified were limited by the extents of LiDAR data or presence of water. In general, faults that are oriented northeast-southwest to east-west are shorter due to the extent of the LiDAR data or presence of water. Additionally, the longer potential faults identified in the study area are also, in general, limited in length by the extent of the LiDAR data or presence of water. Research by Stirling et al. (2013) and Wells and Coppersmith (1994) show that most primary surface fault ruptures occur on faults that are greater than 10 km long. These faults are typically capable of generating earthquakes that exceed magnitude 6 (Stirling et al., 2013; Wells and Coppersmith, 1994). Identifying primary rupture surfaces for earthquakes of magnitude less than 6.0 is difficult (Wells and Coppersmith, 1994).

The individual and composite hillshade images were the most useful data to identify potential faults and lateral offsets across the potential faults. The slope map was also useful in identifying potential fault scarps. Potential faults visible in the hillshade images could typically be seen in the slope and/or aspect maps. DEM data was useful, but often required lots of manipulation to reveal features. The DEM data had to be binned based on the local topography around the features I was attempting to identify. The topographic contour map was the most difficult dataset used to identify potential faults.

The bare-earth LiDAR data was also reviewed for evidence of uplifted marine terraces. Aerial imagery from Bing Maps (Microsoft Corporation, 2013) was reviewed with hillshade and DEM images to approximate the high tide elevation in the study area. Based on my review, the elevation of the high tide is approximately 3 meters. Data published by Archer (1998) shows the relative sea level following the most recent glaciation was approximately 50 meters above the current sea level. Review of the bare-earth LiDAR data revealed a possible paleoshoreline at an elevation of 50 meters along the northwest coast of Kaien Island. The paleoshoreline is approximately 1.2 km long and appears to be level along the length of the feature. None of the potential faults identified intersect the possible paleoshoreline. There are no obvious marine terraces located between the high tide elevation (3 m) and the relative sea level following the most recent glaciation (50 m) that would be useful to identify seismically related post-glacial deformation. There are several relatively flat platforms, not more than approximately 250 km long, located along the slope on the west coast of Kaien Island, south of the paleoshoreline noted above. These platforms may be related glacial processes from the most recent or older glaciations. The platforms are discontinuous along the slope of the west coast of Kaien Island and occur at an elevation of approximately 350 meters.

Potential post-glacial faults were identified according the criteria in the methods section above. The potential post-glacial fault categories were developed to aid in potential field verification. These categories should not be considered an absolute evaluation of the likelihood of these features being potential post-glacial faults. Additionally, not all active faulting may have surficial expressions that are easily identifiable from bare-earth LiDAR data. Faults that do not have obvious topographic expressions may exist within the study area.

8. CONCLUSSIONS

My analysis has identified 80 potential post-glacial faults in the study area that should be field checked. Published research and recorded seismicity in the area suggest that the likelihood of these features being active faults is low. However, previously unknown faults continue to be

discovered around the world and represent a very real hazard. Faults with low recurrence intervals pose a great hazard. Because they have not experienced displacement in recorded history, humans are often unaware of the potential danger. GPS data suggests an accumulation of strain in the vicinity of the study area; however, this does not mean there is active faulting. Additional faulting outside the study area may be present, but was not evaluated as part of my analysis. One such area of concern is the Coast Shear Zone, which is located east of the study area. The Coast Shear Zone can be traced northward to the Denali Fault (Gehrels et al. 2009). The Denali Fault is still considered active today (Gehrels et al., 2009). The Coast Shear Zone was one of the first lineaments identified by researchers in the area and has an orientation consistent with the shear strain in the area (Gehrels et al., 2009; Mazzotti et al., 2008). As noted above, the last activity along the Coast Shear Zone is believed to have occurred approximately 30 Ma (Davidson et al., 2003).

All of the identified potential post-glacial faults should be examined and studied in the field to determine if the identified feature is a fault and potentially active. To reduce risk, additional LiDAR data of more of the surrounding area should be obtained and reviewed. Nearby areas with a more continuous cover over Quaternary deposits may make the identification of post-glacial faults easier. Two such areas that may be of interest are Tugwell Island, located northwest of Digby Island, and a small river valley located between Minerva Lake and the Skeena River, approximately 20 km east of Lelu and Ridley Island. Special interest should also be paid to geophysical studies in the Hecate Strait where the closest earthquake over a magnitude 5.0 was recorded.

9. LIMITATIONS

The study area has a long and complex tectonic and geologic history. There are several documented faults in the area that generally trend northwest to southeast, but published research suggests the faults in the area are inactive. Strain calculations from GPS data discussed above suggest that active faulting in the area may trend northwest-southeast with either right-lateral strike slip movement or dip-slip movement. Linear features that display that orientation and sense of movement would have the highest likelihood of being active faults. However, the history of the site has also led to the development of shear zones and foliations in the area with a similar trend that should be considered inactive. Therefore, categories are highly dependent on visual topographic expressions and professional judgment. If possible, all identified features should be examined in the field to determine if the features are faults. If identified as faults, detailed fault studies should be performed to determine the last time displacement occurred along the fault and if there is a potential for future displacement on the fault.

The recommendations and opinions expressed in this report are based on my review of the background documents referenced below and my visual analysis of the available bare-earth LiDAR data. This evaluation of faulting is limited to the study area shown in Figure 2. Possible faults that were not identified in Figure 13 and that do not have easily identifiable surface expressions may still be present in the study area.

10. SELECTED REFERENCES

Advanced National Seismic System, 2013, ANSS composite earthquake catalog: http://www.ncedc.org/anss/ (last accessed October 22).

Anjen, J.J., Van Staal, C., and Lin, S., 2012, Structural Geology of the Alexander Terrane in the vicinity of Porcher Island, Northwestern British Columbia; *BC Ministry of Energy and Mines*, Geologic Field Work 2011, Paper 2012-1, p. 135-148.

Angen, J., 2013, Structural and geochronological investigation of the southern Alexander terrane in the vicinity of Porcher Island, northwestern British Columbia: M. Sc. Thesis, University of Waterloo, 133 p.

Archer, D.J.W., 1998, Early Holocene landscapes on the north coast of B.C. Canadian Archaeological Association, 31st annual meeting, Victoria, B.C., Abstracts, p. 34.

Barrie, J.V., and Conway, K.W., 1999, Late Quaternary Glaciation and Postglacial Stratigraphy of the Northern Pacific Margin of Canada: *Quaternary Research*, v. 51, Issue 2, p. 113-123.

Barrie, J.V., and Conway, K.W., 2002, Rapid sea-level change and coastal evolution on the Pacific margin of Canada; *Sedimentary Geology*, v. 150, p. 171-183.

Booth, D.B., Troost, K.G., Clague, J.J., and Waitt, R.B., 2003, The Cordilleran Ice Sheet. *In*: Gillespie, A.R., Porter, S.C., and Atwater, B.F.(ed.), *The Quaternary Period in the United States*, *Volume 1*, Developments in Quaternary Science, Elsevier, Volume 1, p. 17-43.

Chardon, D., 2003, Strain partitioning and batholith emplacement at the root of a transpressive magmatic arc; *Journal of Structural Geology*, v. 25, p. 91-97.

Clague, J.J., 1984, Quaternary Geology and Geomorphology, Smithers-Terrae-Prince Rupert Area, British Columbia. Geological Survey of Canada, Ottawa, ON, Memoir 413, 71 pp.

Conway, K.W., Barrie, J.V., and Thomson, R.E., 2012, Submarine slope failures and tsunami hazard in coastal British Columbia: Douglas Channel and Kitimat Arm; *Geological Survey of Canada*, Current Research 2012-10, 13 p.

Crawford, M. L., Crawford, W. A., and Gehrels, G. E., 1999, Terrane assembly and structural relationships in the eastern Prince Rupert Quadrangle, British Columbia, *in* Stowell, H. H., and McClelland, W. C., eds., Tectonics of the Coast Mountains, southern Alaska and British Columbia: Boulder, Colorado, Geological Society of America Special Paper 343.

Cui, Y., Katay, F., Nelson, J.L., Han, T., Desjardins, P.J., and Sinclair, L., 2013, British Columbia Digital Geology; British Columbia Geological Survey, BCGS Open File 2013-04.

Davidson, C., Davis, K.J., Bailey, C.M., Tape, C.H., Singleton, J., and Singer, B., 2003, Age, origin, and significance of brittle faulting and pseudotachylyte along the Coast shear zone, Prince Rupert, British Columbia; *Geology,* January, v. 31, no. 1, p. 43–46, 5 figures.

Gehrels, G.E., Rusmore, M., Woodsworth, G., Crawford, M., Andronicos, C., Hollister, L., Patchett, J., Ducea, M., Butler, R., Klepeis, K., Davidson, C., Friedman, R., Haggart, J., Mahoney, B., Crawford, W., Pearson, D. and Girardi, J., 2009, U-Th-Pb geochronology of the Coast Mountains batholith in north-coastal British Columbia: constraints on age and tectonic evolution; *Geological Society of America Bulletin*, v. 121, p. 1341-1361.

Gottesfeld, A., 1985, Geology of the Northwest Mainland: the geology and paleontology of the Skeena, Nass and Kitimat drainages of British Columbia. Kitimat, BC; Kitimat Centennial Museum Association, 114 pages.

Granger, N., 2001, Kinematics of the Prince Rupert Shear Zone, British Columbia. 14th Keck Geology Symposium Proceedings, p. 85-88.

Haugerud, R.A., Harding, D.J., Johnson, S.Y., Harles, J.L., and Weaver, C.S., 2003, High-resolution Lidar topography of the Puget Lowland, Washington—A bonanza for earth science; *GSA Today*, v. 13, no. 6, p. 4–10.

Hetherington, R., Barrie, J.V., Reid, R.G.B., MacLeod, R., and Smith, D.J., James, T.S., Kung, R., 2003, Late Pleistocene coastal paleogeography of the Queen Charlotte Islands, British Columbia, Canada, and its implications for terrestrial biogeography and early post glacial human occupation; *Canadian Journal of Earth Sciences*, v. 40, p. 1755–1766.

Howle, J.F., Bawden, G.W., Schweickert, R.A., Finkel, R.C., Hunter, L.E., Rose, R.S., and Twistern, B.V., 2012, Airborne LiDAR analysis and geochronology of faulted glacial moraines in the Tahoe-Sierra frontal fault zone reveal substantial seismic hazards in the Lake Tahoe region, California-Nevada, USA; *GSA Bulletin*, v. 124, no. 7/8, p.1087-1101.

Leonard, L. J., R. D. Hyndman, S. Mazzotti, L. L. Nykolaishen, M. Schmidt, and S. Hippchen, 2007, Current deformation in the northern Canadian Cordillera inferred from GPS measurements: *J. Geophys. Res.*, v. *112*.

Massey, N.W.D., MacIntyre, D.G., Desjardins, P.J., and Cooney, R.T., 2005, Digital Geology Map of British Columbia; Whole Province: B.C. Ministry of Energy and Mines, Geofile 2005-1.

Mazzotti, S., H. Dragert, J. Henton, M. Schmidt, R. D. Hyndman, T. James, Y. Lu, and M. Craymer, 2003a, Current tectonics of northern Cascadia from a decade of GPS measurements; *J. Geophys. Res.,* v. 108, p. 2554.

Mazzotti, S., R. D. Hyndman, P. Flück, A. J. Smith, and M. Schmidt, 2003b, Distribution of the Pacific–North America motion in the Queen Charlotte Islands–S. Alaska plate boundary zone; *Geophys. Res. Lett*., v. 30, p. 1762.

Mazzotti, S., Leonard, L. J., Hyndman, R. D., & Cassidy, J. F., 2008, Tectonics, dynamics, and seismic hazard in the Canada-Alaska Cordillera; *Active Tectonics and Seismic Potential of Alaska*, p. 297-319.

Mazzotti, S., Leonard, L.J., Cassidy, J.F., Rogers, G.C., and Halchuk, S., 2011, Seismic hazard in western Canada from GPS strain rates versus earthquake catalog; *J. Geophys. Res*., v. 116.

Microsoft Corporation, 2013, Bing Maps base map for ArcGIS [Computer software]; Redmond, WA (last accessed December 3).

Nelson, J.L., Diakow, J.B., Mahoney, J.B., van Staal, C., Pecha, M., Angen, J., Gehrels, G. and Lau, T., 2012, North Coast project: Tectonics and metallogeny of the Alexander terrane, and Cretaceous sinistral shearing of the western Coast belt; *BC Geological Survey* Geological Fieldwork 2011, 2012-1, p. 157-180.

Stirling, M., Goded, T., Berryman, K., and Litchfield, N., 2013, Selection of Earthquake Scaling Relationships for Seismic-Hazard Analysis; *Bulletin of the Seismological Society of America*, v. 103, no. 6, p. 1-19.

Thackray, G.D., Rodgers, D.W., and Streutker, D., 2013, Holocene scarp on the Sawtooth fault, central Idaho, USA, documented through lidar topographic analysis; *Geology*, v. 41, no. 6, p. 639-642.

Warner, B,.G., Mathewes, R.,W., and Clague, J,.J., 1982, Ice-free conditions on the Queen Charlotte Islands, British Columbia, at the height of late Wisconsin glaciation; *Science*, v. 218, p. 675-677.

Wells, D.L. and Coppersmith, K.J., 1994, New Empirical Relationships among Magnitude, Rupture Length, Rupture Width, Rupture Area, and Surface Displacement; *Bulletin of the Seismological Society of America*, v. 84, no. 4, p. 974-1002.

Wesson, R. L., Frankel, A. D., Mueller, C. S., and Harmsen, S. C., 1999, Probabilistic seismic hazard maps of Alaska: USGS Open File Report 99-35, 43 p.

FIGURES

Scale

0 37.5 75 150 225 300

Kilometers

N W E S

Figure 1: Map of the western coast of British Columbia with study area shown (yellow star). Base map from Bing Maps (Microsoft Corporation, 2013).

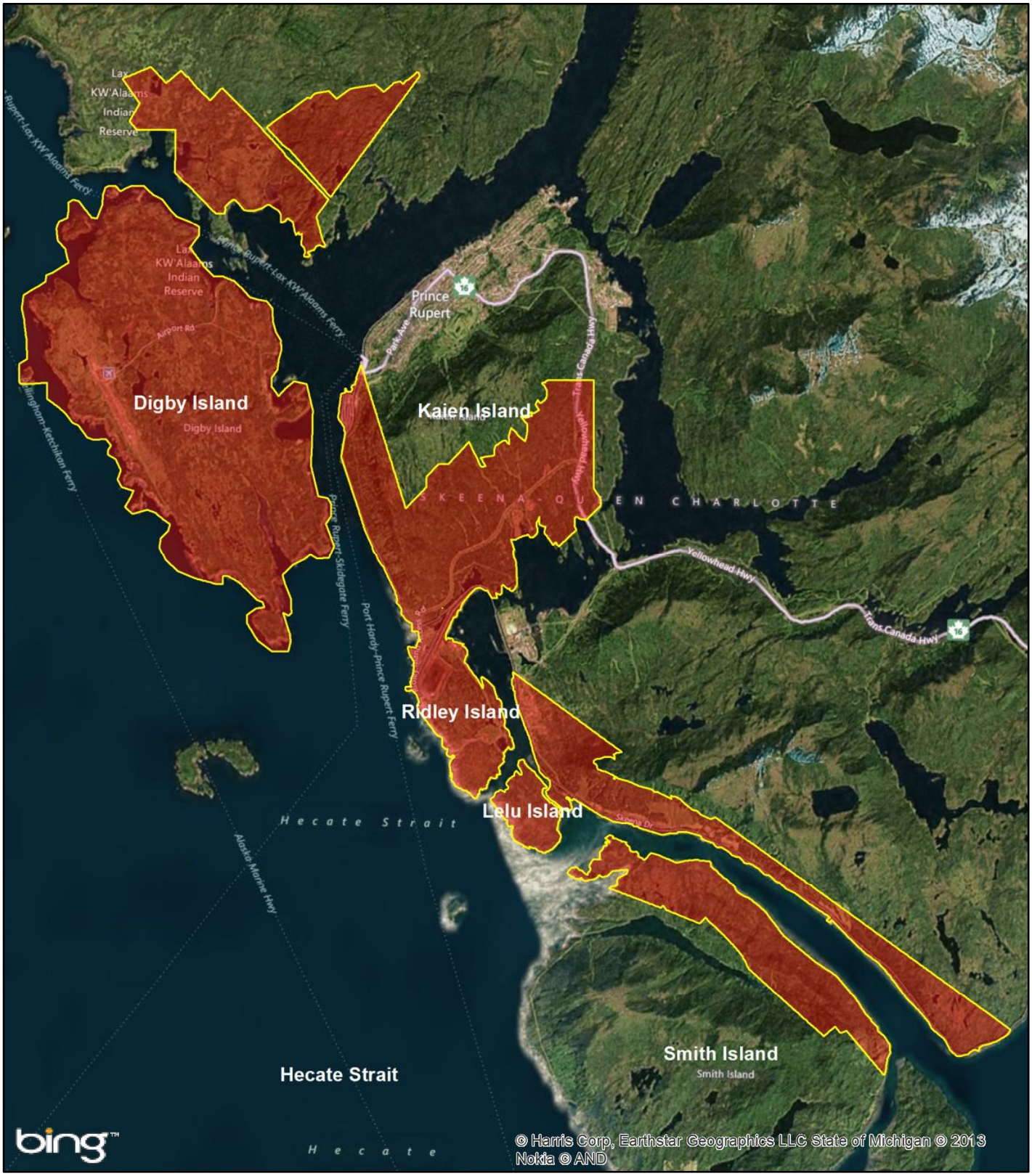

Scale

0 1.25 2.5 5 7.5 10 Kilometers

N W E S

Figure 2: Map of Ridley Island and vicinity with study area shown (shaded red and outlined in yellow). Base map from Bing Maps (Microsoft Corporation, 2013).

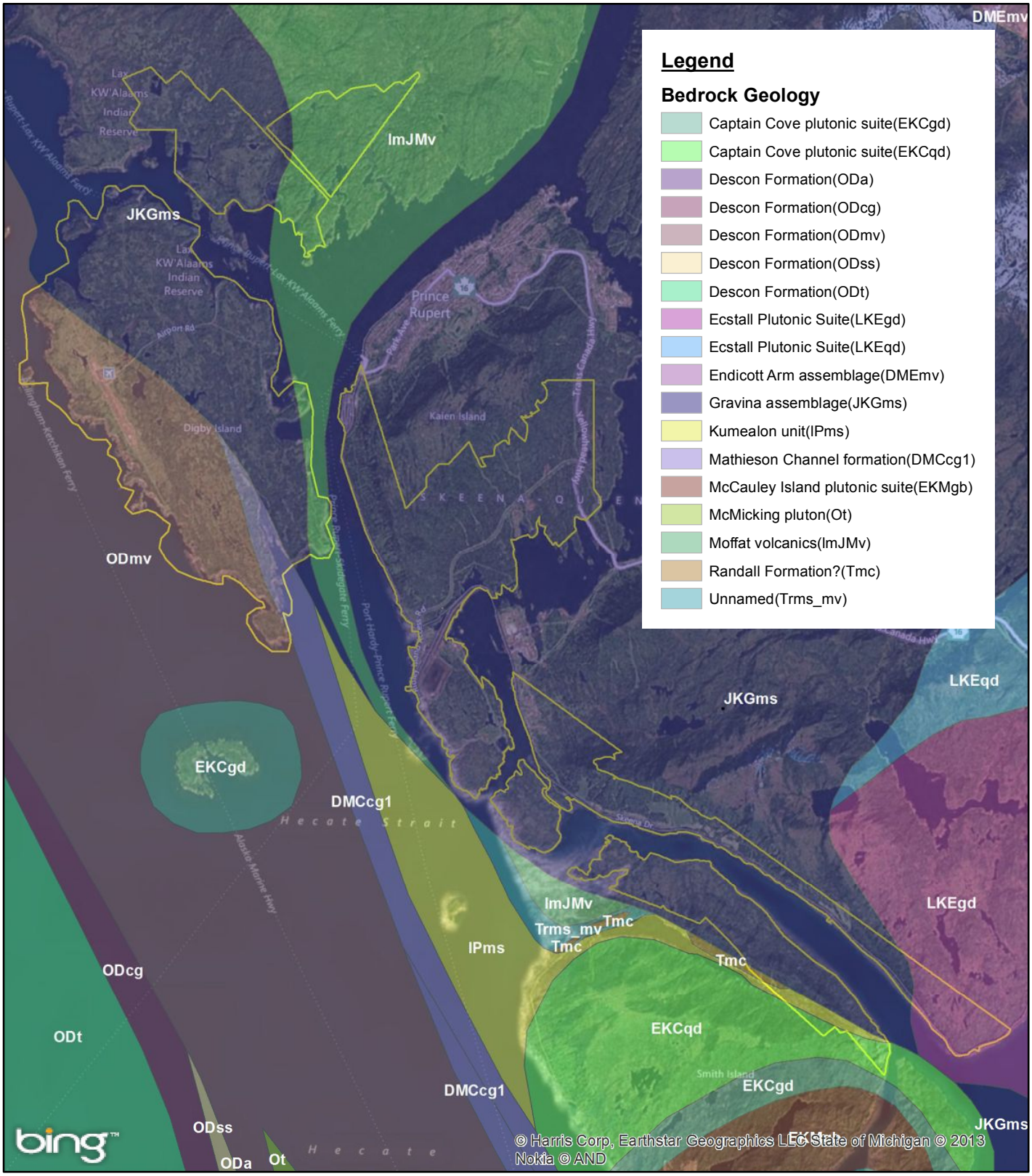

Scale

0 1.25 2.5 5 7.5 10 Kilometers

N W E S

Figure 3: Geologic map of Ridley Island and vicinity with study area shown (yellow outline). Modified from Cui et al., 2013. Base map from Bing Maps (Microsoft Corporation, 2013).

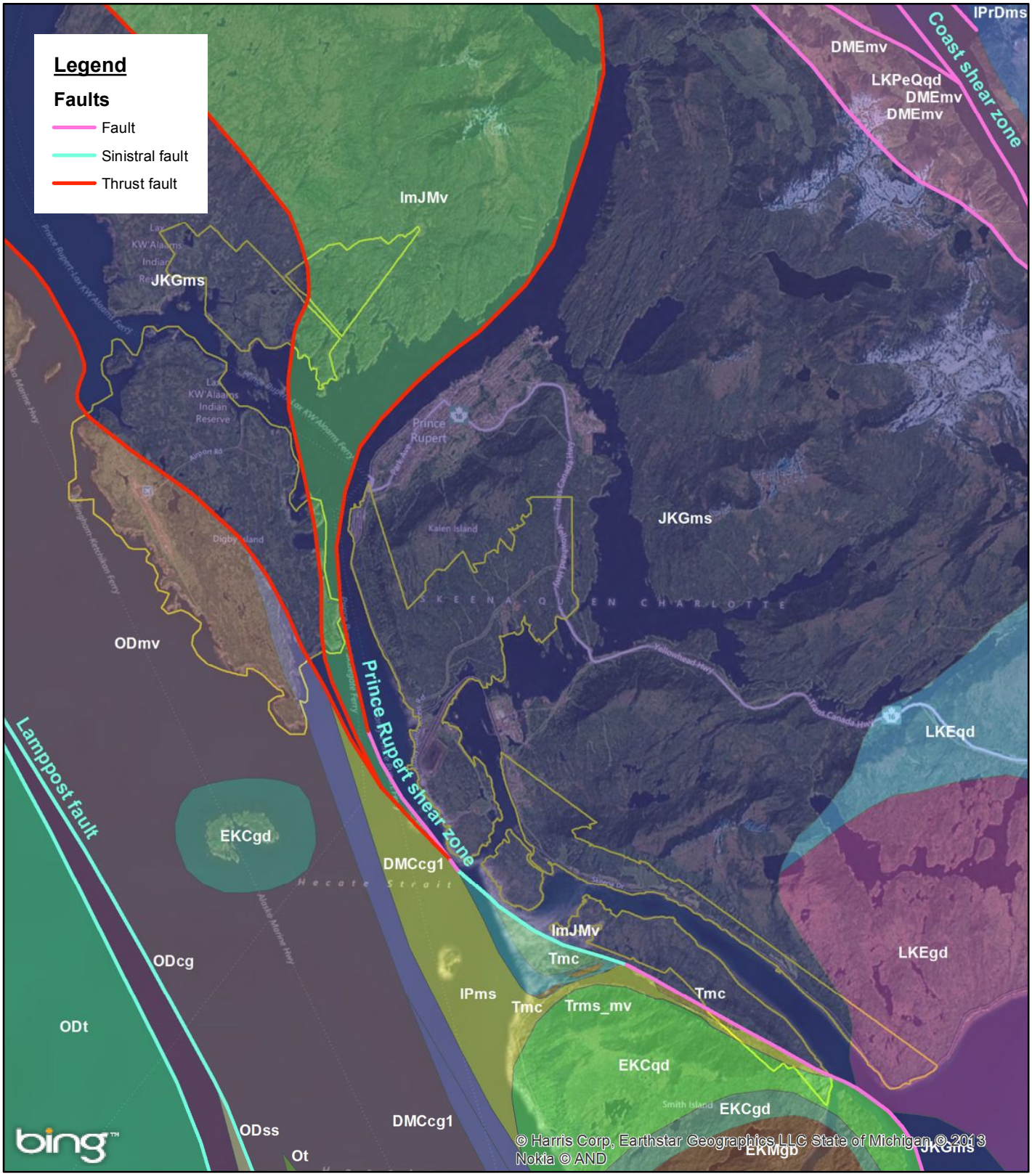

Figure 4: Geologic map showing faults in relationship to the study area (yellow outline). Modified from Cui et al., 2013. Base map from Bing Maps (Microsoft Corporation, 2013).

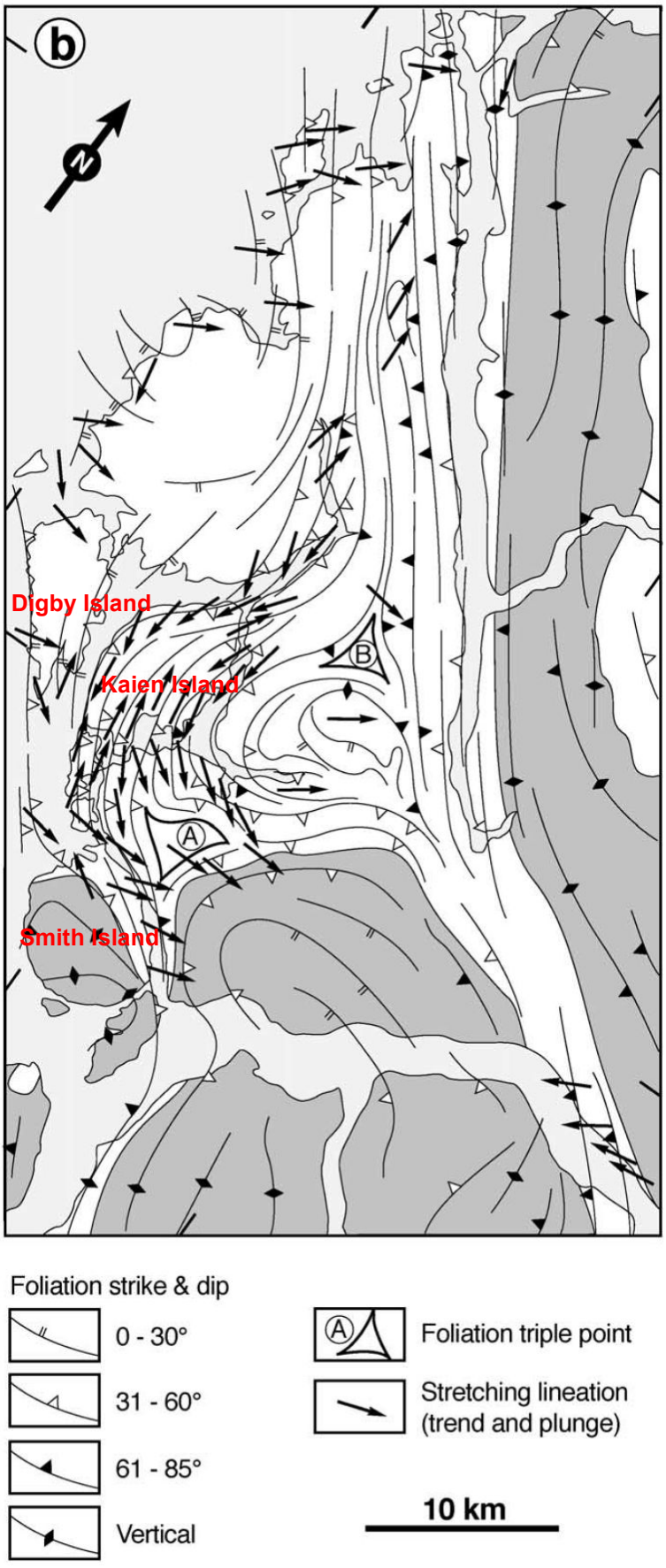

Figure 5: Structural map of the Prince Rupert area from Chardon (2003). Foliations based on measurements and photointerpretations. Select island locations indicated in red.

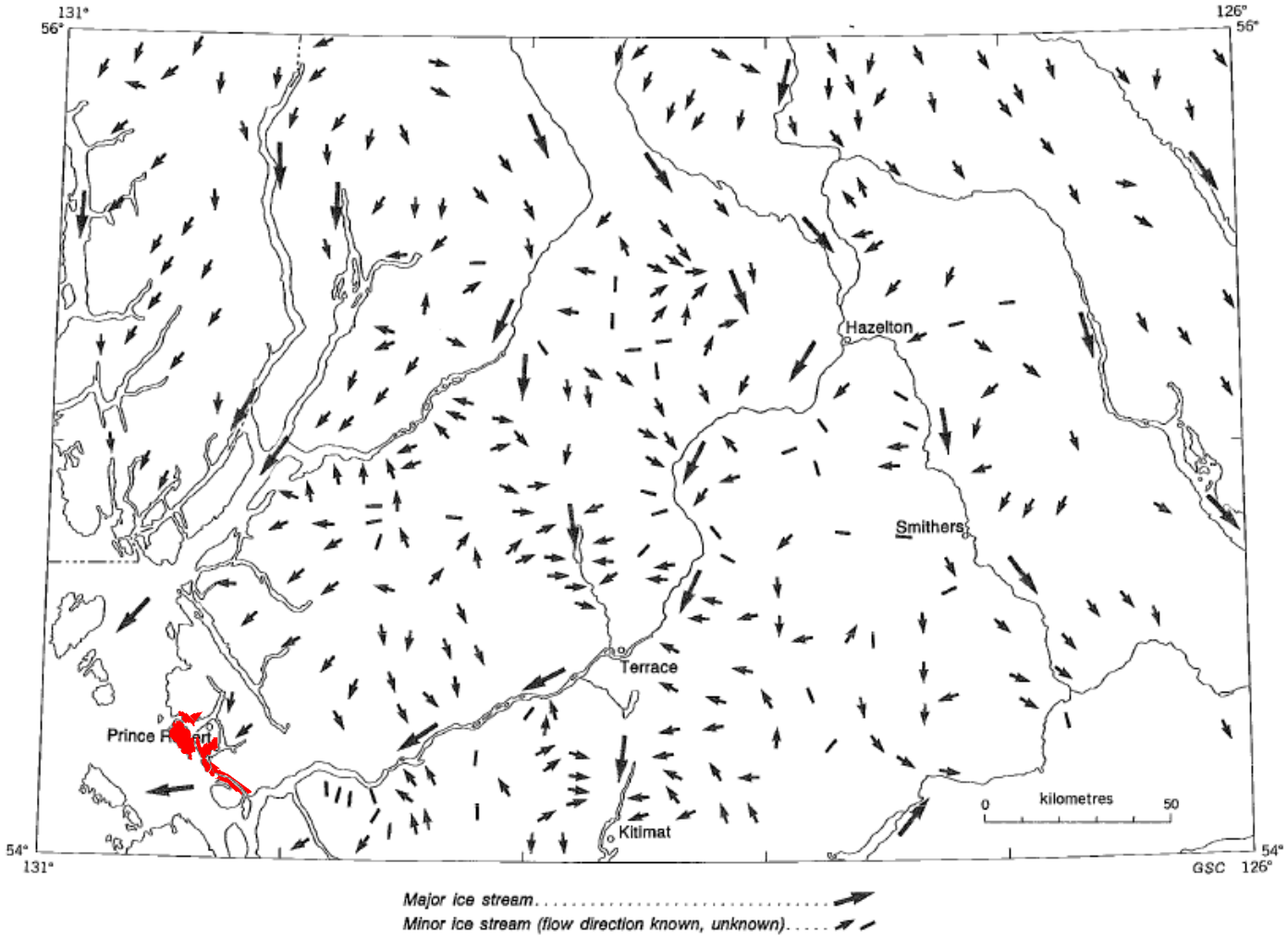

Figure 40. *Pattern of glacier flow during the Fraser Glaciation.*

Figure 6: Glacial flow map during the Frasier Glaciation from Clague (1984). Valleys and lowlands were covered by the Frasier ice sheet. Approximate location of study area shown in red.

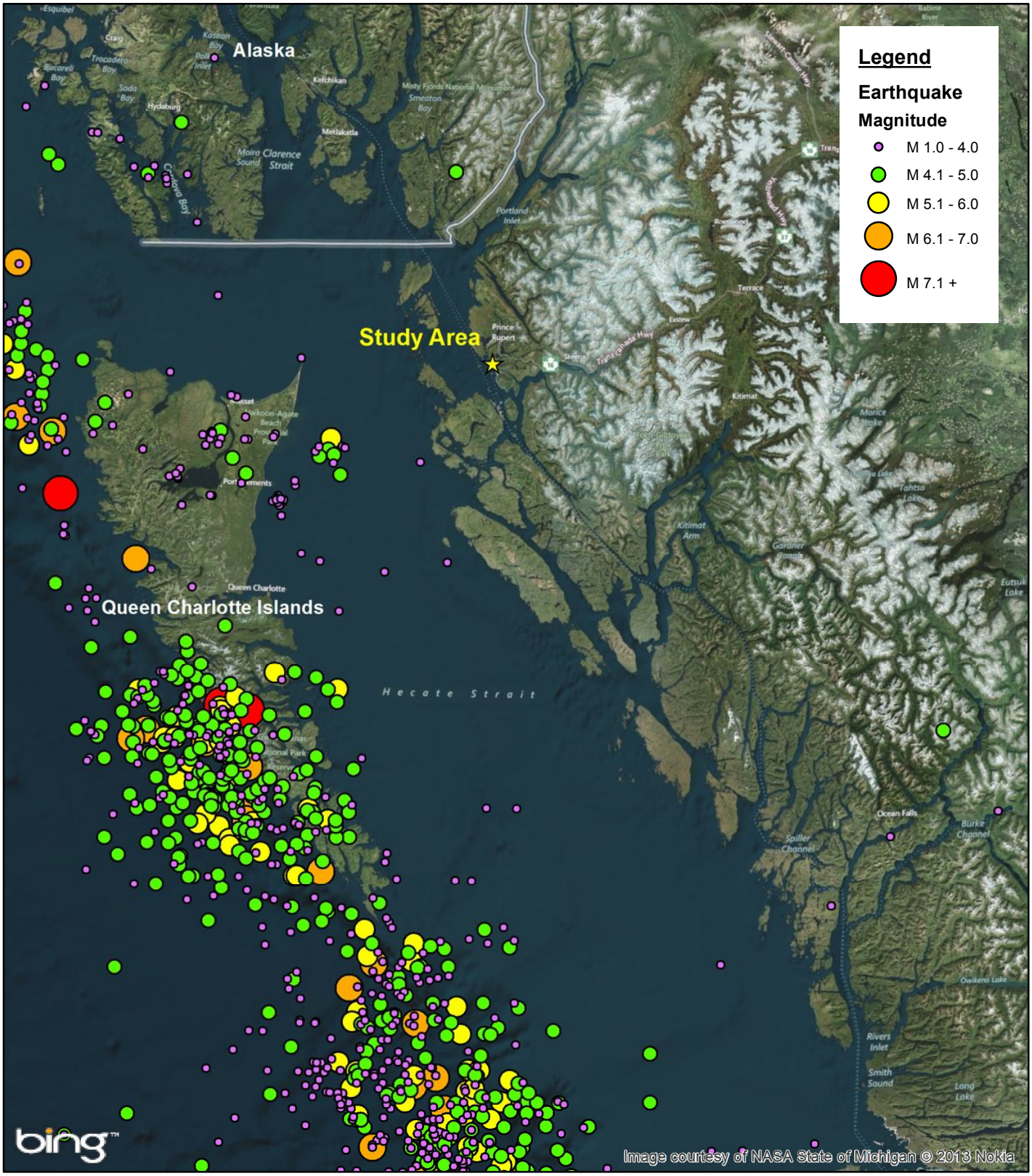

Scale

0 25 50 100 150 200 Kilometers

N W E S

Figure 7: Earthquakes recorded along the north and central coast of British Columbia since 1898. Modified from Advanced National Seismic System, 2013. Base map from Bing Maps (Microsoft Corporation, 2013).

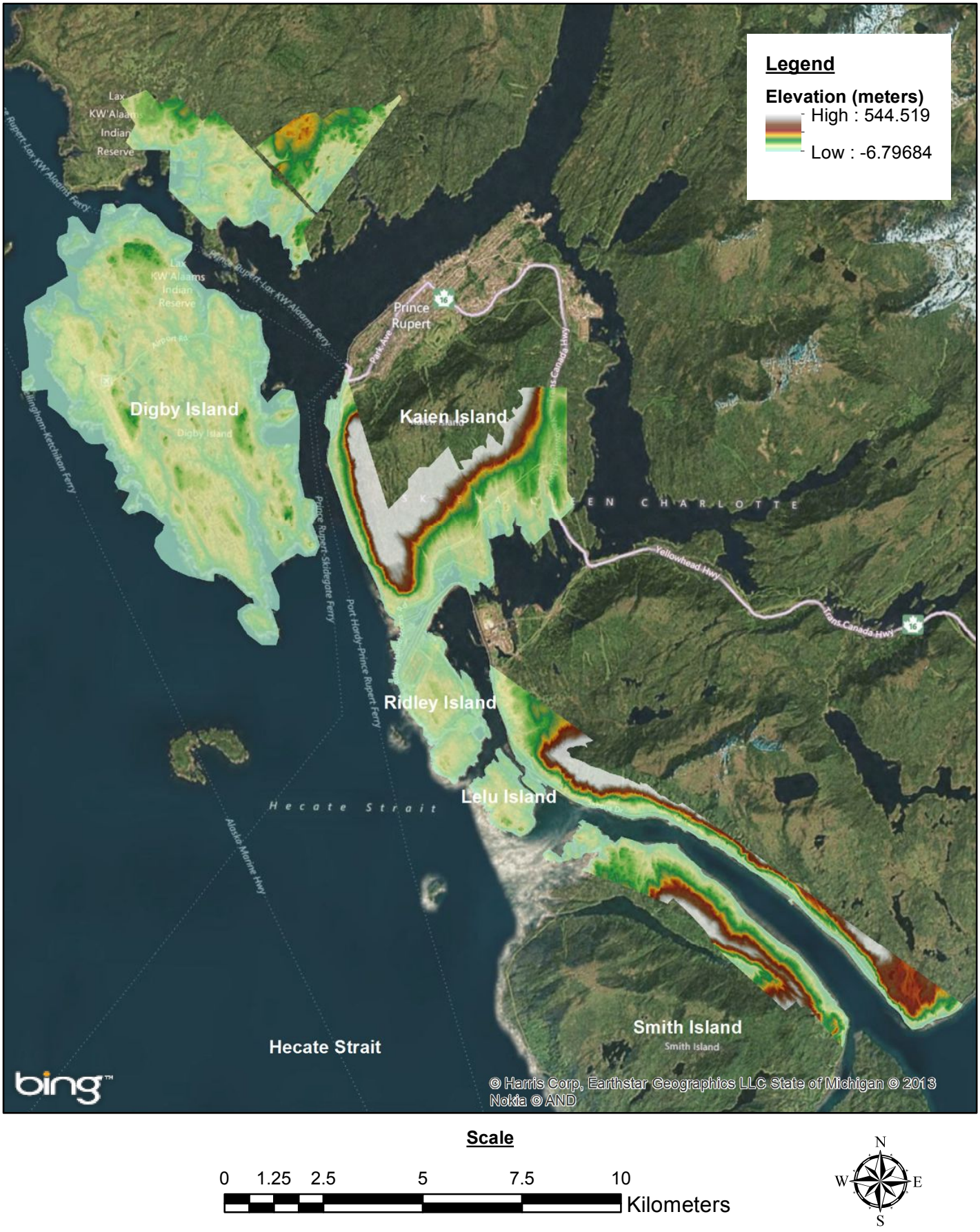

Scale

0 1.25 2.5 5 7.5 10 Kilometers

N W E S

Figure 8: Digital elevation model (DEM) of the study area.
Base map from Bing Maps (Microsoft Corporation, 2013).

Scale

0 1.25 2.5 5 7.5 10 Kilometers

N
W E
S

Figure 9: Hillshade map of Ridely Island and vicinity. The map shown is a composite of four partially transparent hillshade images with solar illumination angles of 45, 135, 225, and 315 degrees. Hillshade images derived from DEM of the study area. Base map from Bing Maps (Microsoft Corporation, 2013).

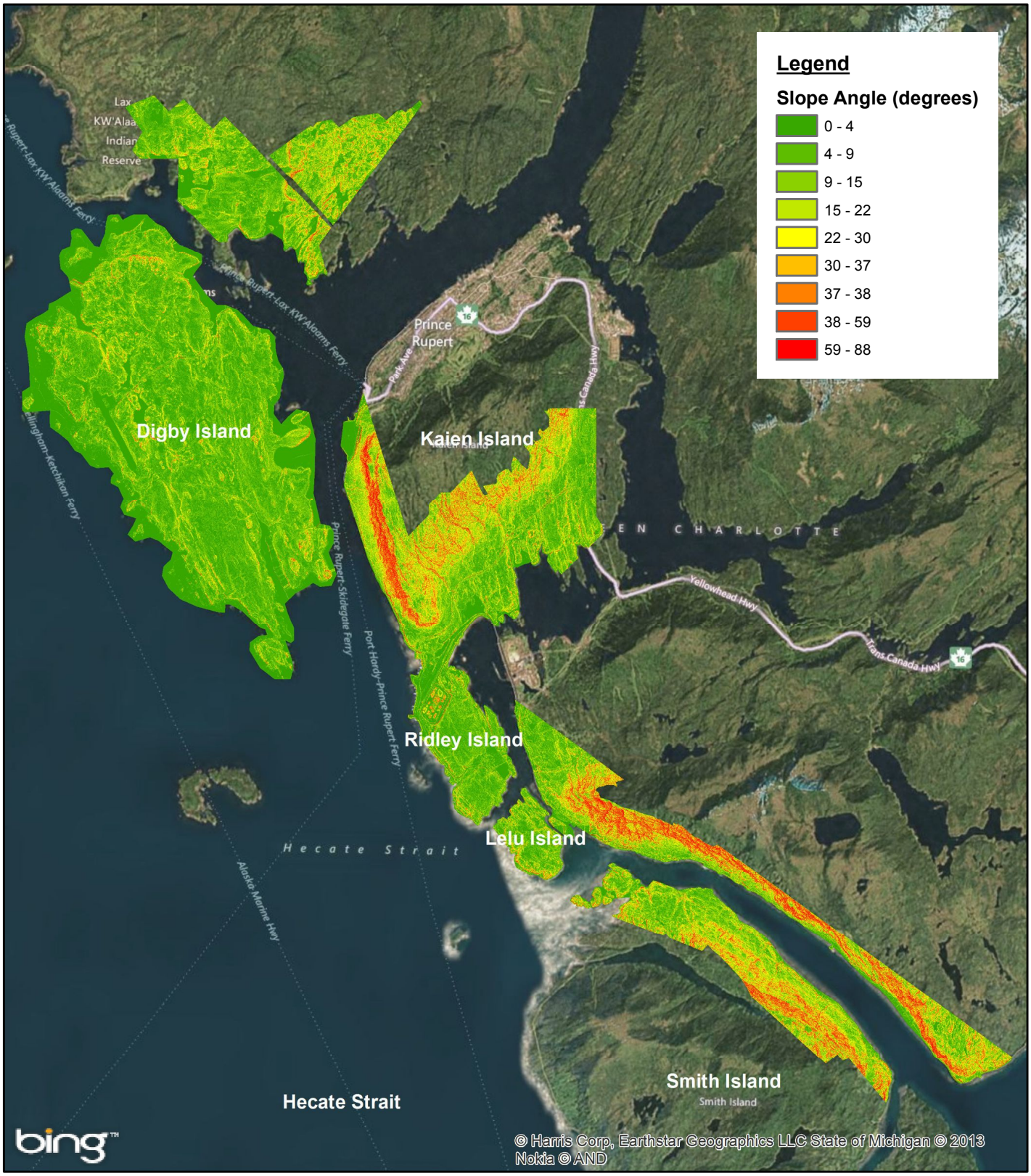

Scale

0 1.25 2.5 5 7.5 10 Kilometers

N
W E
S

Figure 10: Slope map of Ridely Island and vicinity. Map derived from DEM of the study area. Base map from Bing Maps (Microsoft Corporation, 2013).

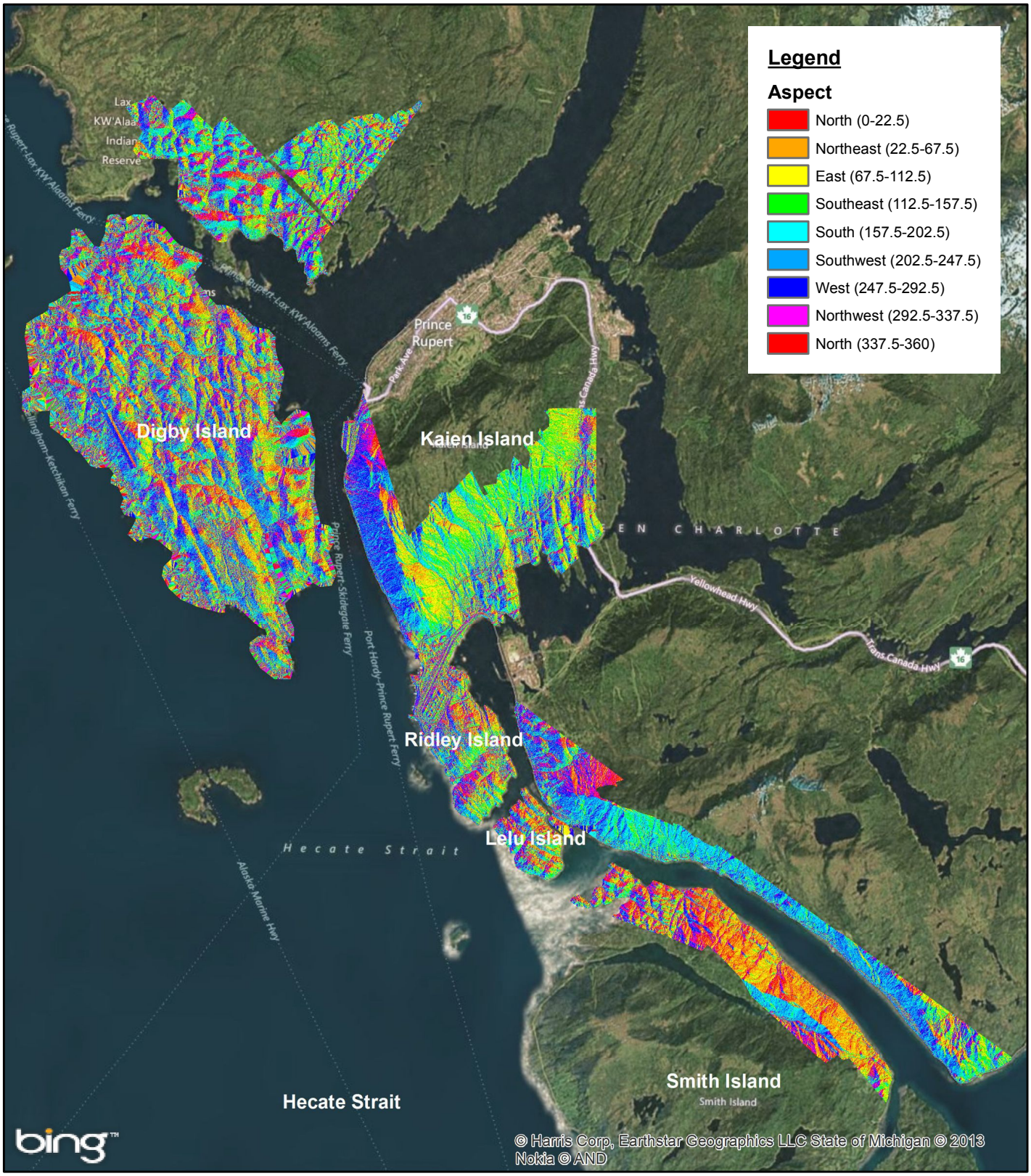

Scale

0 1.25 2.5 5 7.5 10 Kilometers

N W E S

Figure 11: Aspect map of Ridely Island and vicinity. Map derived from DEM of the study area. Base map from Bing Maps (Microsoft Corporation, 2013).

Scale

0 1.25 2.5 5 7.5 10 Kilometers

N W E S

Figure 12: Topographic contour map of Ridley Island and vicinity. Contours overlayed onto the composite hillshade map and derived from DEM of the study area. Base map from Bing Maps (Microsoft Corporation, 2013).

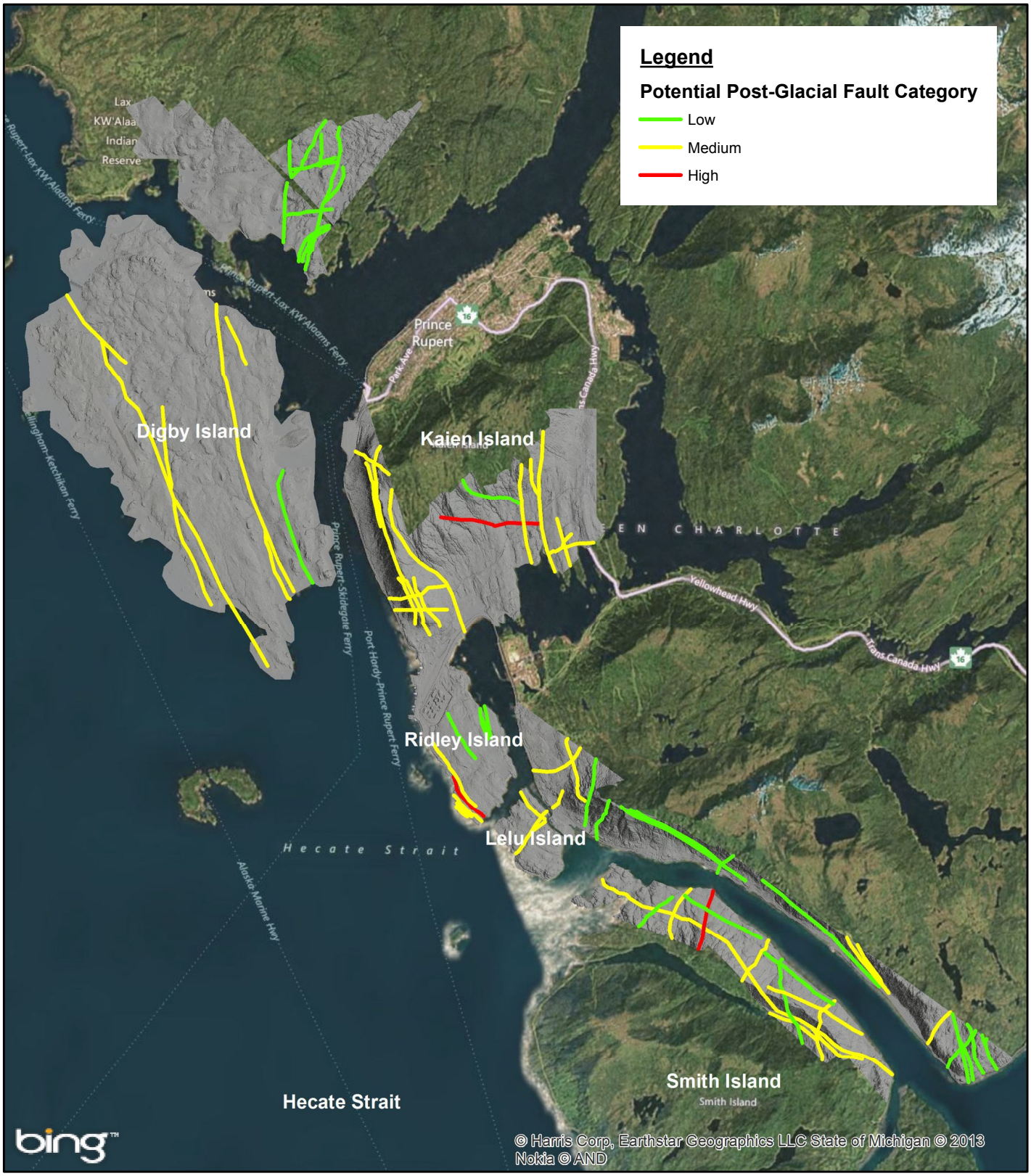

Scale

0 1.25 2.5 5 7.5 10 Kilometers

N W E S

Figure 13: Potential post-glacial fault map overlayed onto the composite hillshade map. Faults are categorized into three categores based on the potential of the feature being a post-glacial fault. Base map from Bing Maps (Microsoft Corporation, 2013).

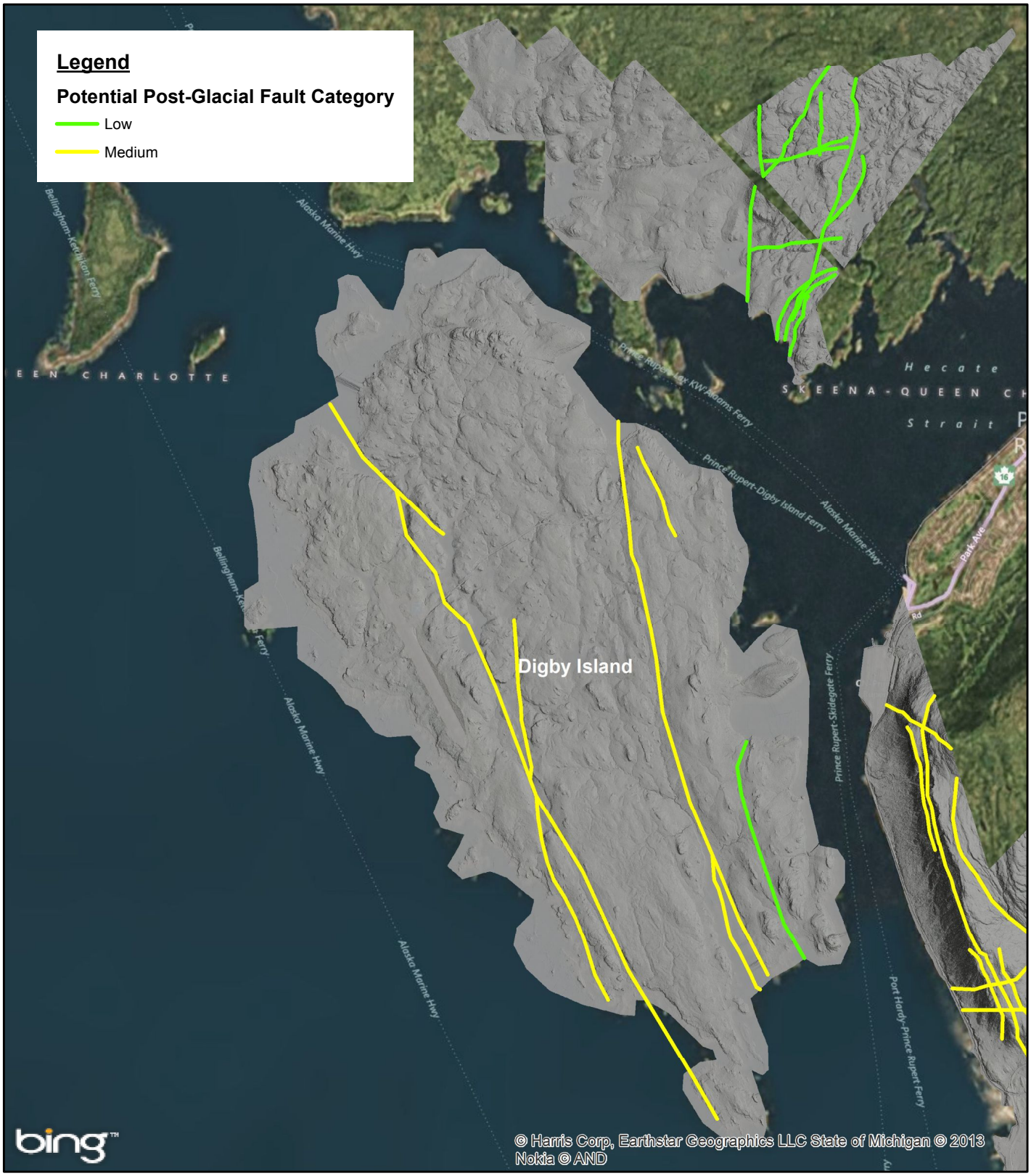

Scale

0 0.5 1 2 3 4 Kilometers

N W E S

Figure 14: Close-up of the Digby Island and northern B.C. mainland area from Figure 13. Base map from Bing Maps (Microsoft Corporation, 2013).

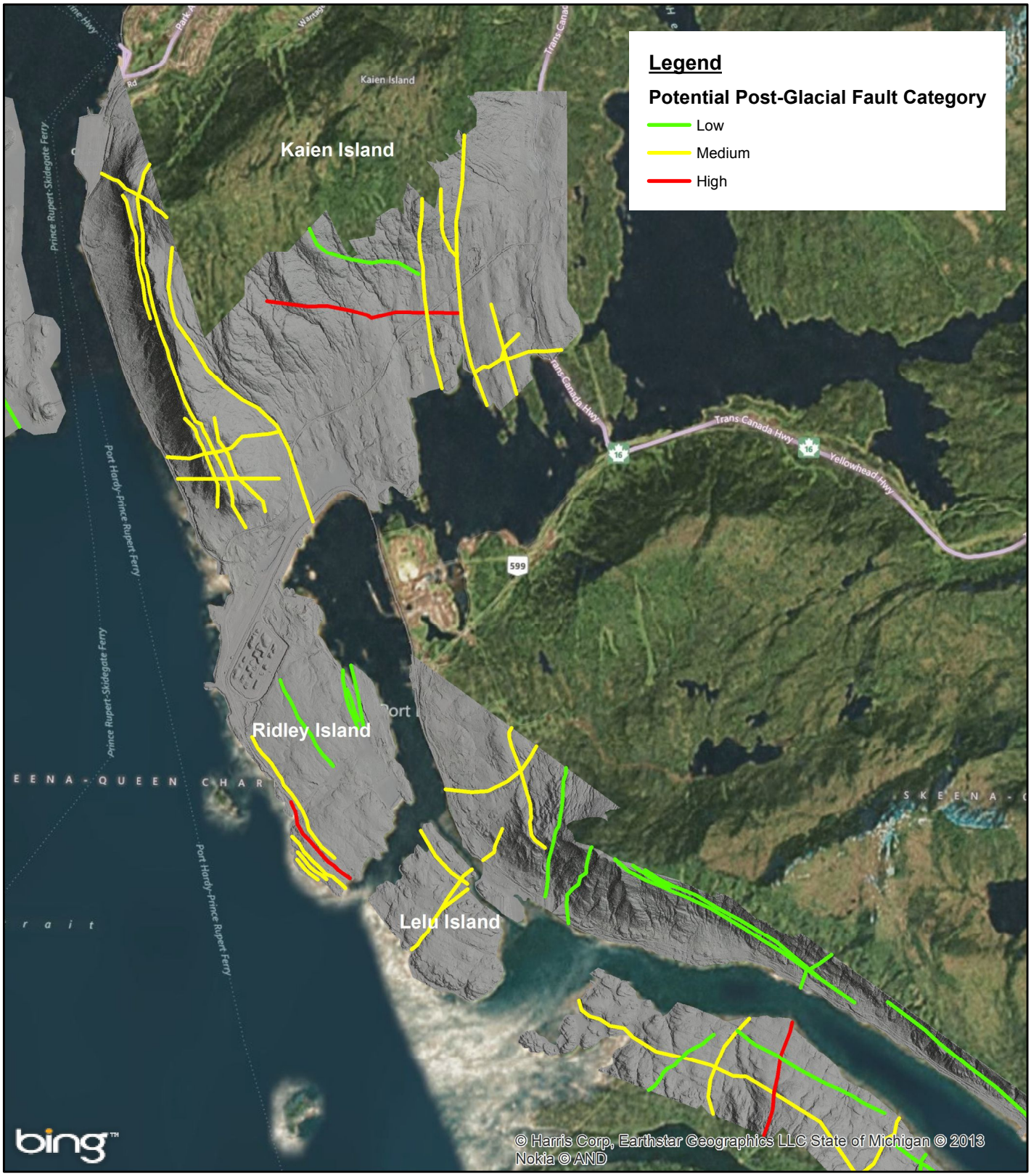

Scale

0 0.5 1 2 3 4 Kilometers

N W E S

Figure 15: Close-up of Kaien, Ridley and Lelu Islands from Figure 13.
Base map from Bing Maps (Microsoft Corporation, 2013).

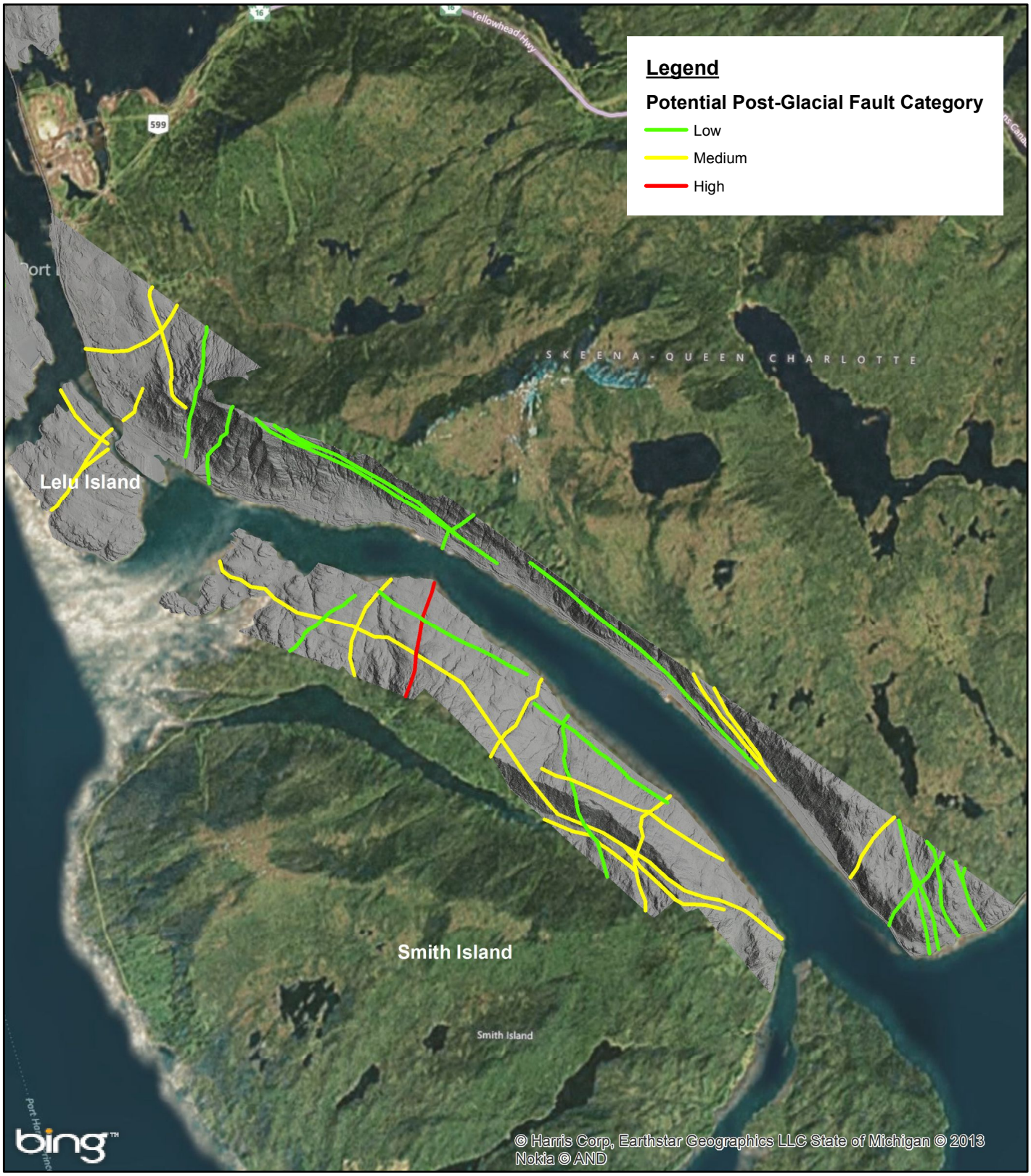

Scale

0 0.5 1 2 3 4 Kilometers

N
W E
S

Figure 16: Close-up of Smith Island and southern B.C. mainland area from Figure 13. Base map from Bing Maps (Microsoft Corporation, 2013).